

Stem Cell Reports, Volume 12

Supplemental Information

**Therapeutic Regeneration of Lymphatic and Immune Cell Functions
upon Lympho-organoid Transplantation**

Elisa Lenti, Silvia Bianchessi, Steven T. Proulx, Maria Teresa Palano, Luca Genovese, Laura Raccosta, Antonello Spinelli, Denise Drago, Annapaola Andolfo, Massimo Alfano, Tatiana V. Petrova, Sylvain Mukenge, Vincenzo Russo, and Andrea Brendolan

SUPPLEMENTAL EXPERIMENTAL PROCEDURES

Transplantation under kidney capsule and at axillary/popliteal region

Pre-LOs were kept on ice and transplanted *in vivo*. The transplantation at the renal subcapsular space of the right kidney of anesthetized C57BL/6 mice was performed as previously described. Three-four weeks later, LOs were harvested, fixed and stained for immunofluorescence analysis (Suematsu and Watanabe, 2004). For pre-LOs transplantation at axillary region: C57BL6/N were anesthetized and intradermal injection of 3% Evans blue solution (Sigma) into the palmar side of the forelimb footpad was performed to detect LNs. Then axillary/brachial LNs were resected within a small portion of the surrounding fat pad and of the lymphatic vessels. Immediately after the LNs removal, LOs were transferred or not at site of resection, and LOs were kept at the site by closing the fat pad pocket with suture. For sham-operated mice, skin was opened and immediately sutured. Two months after, lymphatic drainage analysis through *in vivo* planar optical and μ CT imaging was performed. For pre-LOs transplantation at popliteal region: C57BL6/ and Prox1-mOrange mice were anesthetized, popliteal LNs (LN) were resected and pre-LOs were transferred or not at site of resection. As for transplantation at axillary region, LOs were kept inside the fat pad pocket with suture, and in sham-operated mice skin was opened and immediately sutured. One month after, lymphatic perfusion analysis was performed, then LOs were collected, fixed and analysed by immunofluorescence staining.

Immunohistochemistry, immunofluorescence and confocal analyses of LOs

Pre-LOs and LOs after 3-4 weeks from transplantation were harvested and fixed 5 minutes at 4°C with 4% (wt/vol) PFA (Sigma-Aldrich), then washed in PBS 1X and dehydrated overnight in 30% sucrose (Sigma-Aldrich) at 4°C. Samples were embedded in Tissue-Tek OCT compound (Bio-Optica) and frozen in an ethanol dry-ice bath. Eight- to ten-micrometer-thick sections were placed onto glass slides (Bio-Optica), fixed in cold acetone for 5 minutes, dried, and kept at -80°C until used. Slices were incubated 30 minutes with a blocking solution of PBS at 0.5% FBS and 0.05% Tween (PBS-T), followed by anti-CD3 (PE hamster IgG1 κ ; 130-102-792, clone 145-2C11; 1:300 stock 30 μ g/ml; Miltenyi), anti-CD45R/B220 (biotin rat IgG2a, κ ; 553085, clone RA3-6B2; 1:100 stock 0.5 mg/ml; BD), anti-CD31/PECAM-1 (PE rat IgG2a; 553373, clone MEC 13.3; 1:100 stock 0.2 μ g/ μ l; BD), anti-LYVE-1 (rabbit IgG; NB600-1008; 1:600 stock 1 mg/ml; Novusbio), anti-RFP (rabbit IgG; 600-401-379; 1:600 stock 1.1mg/ml; Rockland), anti-GFP (chicken IgG; ab13970; 1:250 stock 10mg/ml; Abcam), anti-CD35 (biotin rat IgG2a, κ ; 553816, clone 8C12; 1:100 stock 0.5 mg/ml; BD) and anti-COLL-IV alpha 1 (rabbit IgG; NB120-6586; 1:500 stock 1 mg/ml; Novusbio) specific antibodies diluted in PBS-T blocking solution. Secondary anti-rabbit Alexa

Fluor 488 (1:250 stock 2 $\mu\text{g}/\mu\text{l}$; A21206; Invitrogen), anti-rabbit Alexa Fluor 647 (1:250 stock 2 $\mu\text{g}/\mu\text{l}$; A31573; Invitrogen), anti-rat Alexa Fluor 546 (1:250 stock 2 $\mu\text{g}/\mu\text{l}$; A11081; Invitrogen), anti-chicken Alexa Fluor 488 (1:250 stock 2 $\mu\text{g}/\mu\text{l}$; A11039; Invitrogen), anti-rabbit Alexa Fluor 546 (1:250 stock 2 $\mu\text{g}/\mu\text{l}$; S11223; Invitrogen), was diluted in PBS-T blocking solution and incubated for 30 minutes. Nuclei were visualized with DAPI (Fluka) and mounting was performed with Mowiol (Calbiochem). Images were acquired using an Ultraview Leica TCS SP8 laser confocal microscope and Zeiss AxioObserver.Z1. Digital images were recorded in separately scanned channels with no overlap in detection of emission from the respective fluorochromes. Final image processing was performed with Adobe Photoshop and Illustrator and minimal contrast and luminosity adjustment.

In vivo planar, 3D and μCT optical imaging

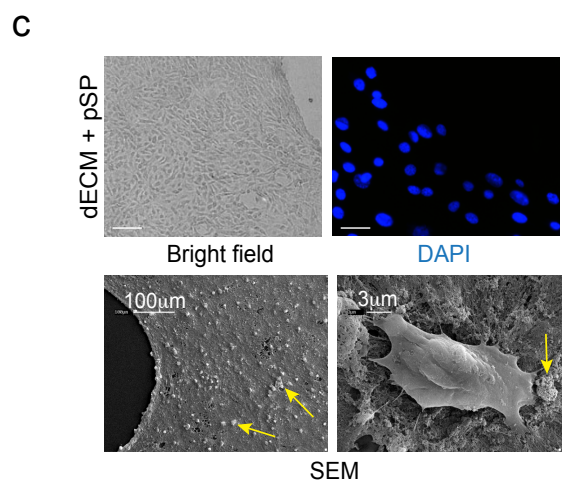
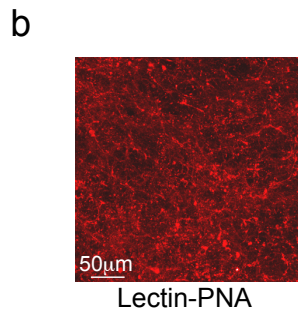
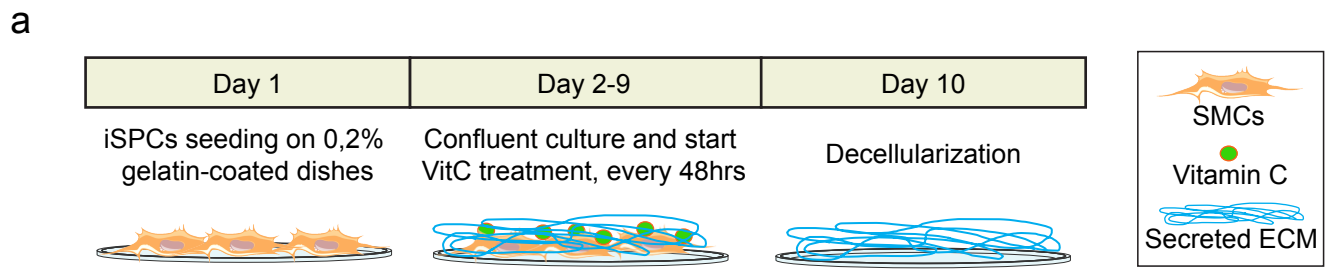
In vivo planar (2D) fluorescence imaging (FLI) was performed using an IVIS SpectrumCT imaging system (Perkin Elmer). The system is equipped with a low noise, back-thinned, back-illuminated CCD camera cooled at $-90\text{ }^{\circ}\text{C}$. Each mouse was s.c injected with $5\mu\text{l}$ of $20\mu\text{M}$ P20D800 lymphatic tracer at dorsal paw immediately prior to FLI (see Figure 2a). Dynamic FLI was performed by acquiring a set of images every 2 minutes from 0 to 10 minutes after tracer injection to detect the maximum FLI signal in the LNs region. The images were obtained using the following IVIS settings: exposure time=auto, binning=8, f=1 and a field of view equal to 12 cm (field C).

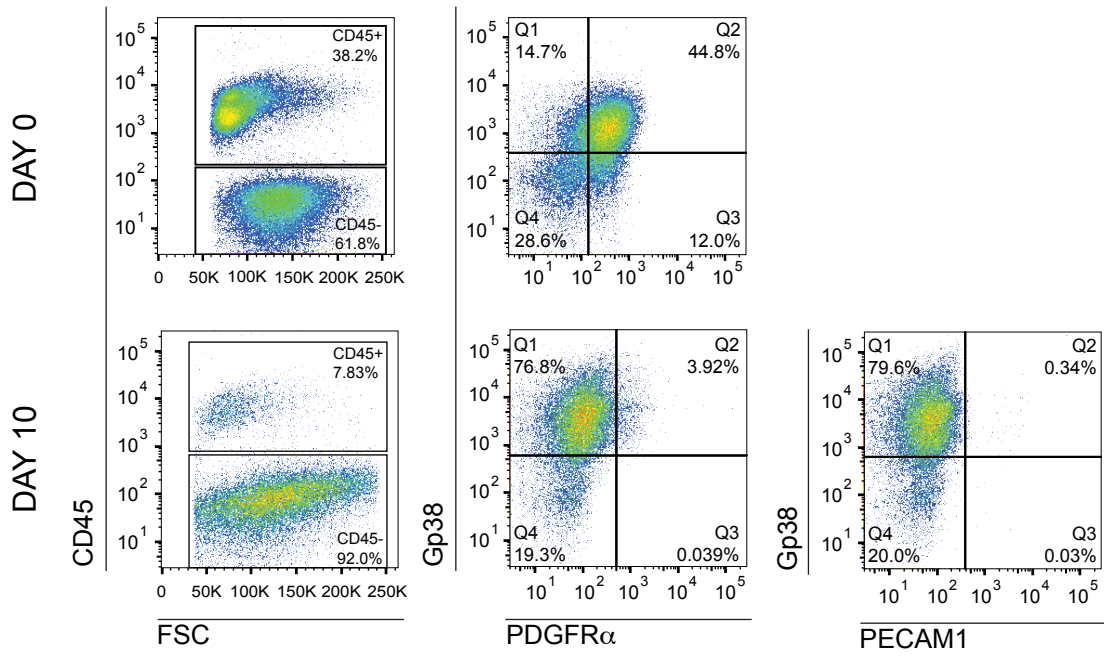
Excitation/Emission=745/840 filters were used for epi-illumination FLI acquisitions. During image acquisition, the animals were kept at $37\text{ }^{\circ}\text{C}$ and under inhalation anaesthesia (2–3% isoflurane and 1 l/min O_2). FLI images were acquired and analysed using Living Image 4.5 (Perkin Elmer). ROI values were processed using GraphPad Prism 5 (GraphPad Software Inc.).

In vivo μCT imaging was performed using the IVIS SpectrumCT, μCT images were acquired without any contrast medium, with the following parameters: x-ray tube voltage=50 kV, tube current=1 mA, x-ray focal spot size=50 μm . The μCT images calibrated in Hounsfield unit (HU) were reconstructed with a voxel size of $75\text{ }\mu\text{m}^3$. Tomographic fluorescence imaging (FLIT) was performed 10min after P20D800 injection (immediately after the last FLI image) using transillumination with the same acquisition parameters used for epi-illumination and the reconstructed 3D images were fused with μCT images using Living Image 4.5.

Perfusion analysis of popliteal collecting lymphatic vessels

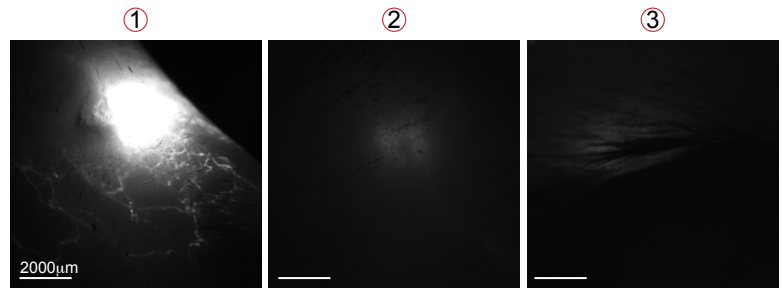
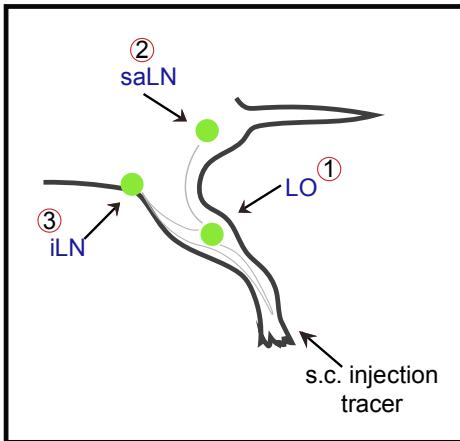
Assessment of the perfusion of lower limb collecting lymphatic vasculature using NIR fluorescence imaging was performed as previously described (Proulx et al., 2017). In brief, a Zeiss StereoLumar.V12 microscope adapted for sensitivity in NIR wavelengths was used to acquire videos to assess lymphatic perfusion during injection of 5 μ l of 20 μ M P20D680 into the dorsal skin of the rear paw. Videos were recorded for 3 min and were subsequently scored for perfusion of tracer to the afferent collecting lymphatic vessels entering the popliteal region, the efferent collecting lymphatic vessels exiting the popliteal region and within the sacral LNs. To score the perfusion of AV, EV and saLN, all the recorded videos were watched and all parameters evaluated separately; a positive score was assigned when the perfusion with the dye was observed. If backflow of tracer to the dermal lymphatic vessels near the paw was observed this was also recorded. For lymphatic perfusion experiments, *Prox1-mOrange2* mice were anesthetized and injected with 5 μ l of 8 μ g/ μ l dextran-FITC (cat.no. FD2000S, Sigma) into the dorsal skin of the rear paw. Images were acquired using Zeiss Axio Zoom V16 fluorescence microscope, recorded in separately scanned channels with no overlap in detection of emission from the respective fluorochromes. Final image processing was performed with Adobe Photoshop and Illustrator and minimal contrast and luminosity adjustment.



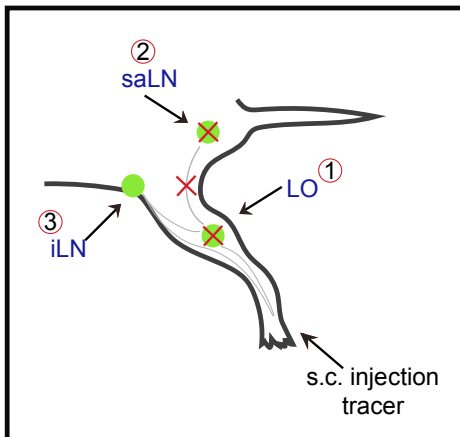


Imaging perfusion: Scheme of analysis and videos recording steps.

Imaging perfusion: LO transplanted



Imaging perfusion: CTRL (popLN resected)



To score the perfusion of AV, EV and saLN, all the recorded videos were watched and all parameters evaluated separately. A positive score was assigned when the perfusion with the dye was observed. For quantification analysis of saLN perfusion, a positive score was assigned if the saLN was perfused by the NIR dye. If backflow of tracer to the dermal lymphatic vessels near the paw was observed this was also recorded.

Supplemental Figure 1. ECM-based scaffold supports cell adhesion, Related to Figure 1

- a) Scheme for generating ECM within 10 days. Vitamin C was added to the culture every two days and then decellularized at day 10.
- b) Representative confocal images of Lectin-PNA staining of dECM.
- c) Representative bright field, confocal images (upper panel), and scanning electron microscopy (lower panel) of dECM with stromal progenitor cells. DAPI staining indicate nuclei; yellow arrows indicate glycosaminoglycan aggregates. Scale bars = 25um (bright field and DAPI), 100uM and 3uM (SEM=scanning electron microscopy).

Supplemental Figure 2. Phenotypic characterization of LN stromal progenitors, Related to Figure 1.

Representative FACS plot analysis of primary stromal progenitors obtained from neonatal mesenteric LNs before (Day 0) and after (Day 10) ex vivo expansion. Antibodies against CD45, GP38, PDGFR-a and PECAM-1 were used to assess phenotype of cells.

Supplemental Figure 3. Scheme of imaging analysis and videos recording, Related to Figure 3.

To score the perfusion of AV, EV and saLN, all the recorded videos were watched and all parameters evaluated separately. A positive score was assigned when the perfusion with the dye was observed. For quantification analysis of saLN perfusion, a positive score was assigned if the saLN was perfused by the NIR dye. If backflow of tracer to the dermal lymphatic vessels near the paw was observed this was also recorded.

Table 1. List of proteins resulted from mass-spectrometry analysis

List of total proteins in dSPL and dECM common to mouse matrisome			
Proteins common between dSPL and dECM		Proteins present in dSPL only	Proteins present in dECM only
Name	Name	Name	Name
WISP2	LOXL1	COCH	FBLN2
EMILIN2	TGM2	FGA	PCOLCE
FN1	LOX	FGG	EFEMP2
TNC	ADAMTSL4	LAMA2	TSKU
TGFBI	P4HA1	LAMA4	VCAN
FGB	SERPINH1	LAMB1	COL4A5
TINAGL1	CTSB	LTBP4	COL4A6
FBLN5	LGALS1	MMRN1	P4HA2
NID1	LGALS3	SBSPON	CTSL
AGRN	COLEC12	THBS1	PLOD3
EFEMP1	ANXA2	DPT	SERPINF1
MATN2	ANXA5	FGL2	ANXA1
EMILIN1	LGALS9	LTBP2	ANGPTL4
FBN1	MFGE8	MFAP4	NGF
POSTN	S100A4	MFAP5	S100A6
LAMB2	ANGPTL2	VTN	
LAMC1	HCFC1	VWA1	
LAMA5	PLXNB2	LUM	
TNXB		OGN	
NID2		COL15A1	
ASPN		COL6A4	
HSPG2		COL6A5	
DCN		COL6A6	
PRELP		ITIH1	
BGN		ITIH2	
COL3A1		SERPINA1C;1A	
COL5A3		CTSG	
COL18A1		ELANE	
COL14A1		SERPINA1B	
COL12A1		SERPINA1D	
COL5A1		SERPINA1E	
COL16A1		SERPINA3K	
COL1A1		ANXA7	
COL5A2		LMAN1	
COL1A2		PF4	
COL6A3		IL16	
COL4A1		S100A10	
COL6A2		S100A13	
COL6A1		S100A9	
COL4A2		TGFB1	

Glycoproteins
Proteoglycans
Collagens
ECM Regulators
ECM Affiliated
Secreted factors

Statistically significant (p<0.01) between dSPL vs dECM

Proteins common between dSPL and dECM		Proteins present in dSPL only	Proteins present in dECM only
Name	Name	Name	Name
WISP2	LOXL1	COCH	FBLN2
EMILIN2	TGM2	FGA	PCOLCE
FN1	LGALS1	FGG	P4HA2
TNC	MFGE8	LAMA2	ANXA1
TGFBI		LAMA4	ANGPTL4
FGB		LAMB1	
TINAGL1		LTBP4	
FBLN5		MMRN1	
NID1		SBSPON	
AGRN		THBS1	
ASPN		COL15A1	
HSPG2		COL6A4	
DCN		COL6A5	
COL3A1		COL6A6	
COL5A3		ITIH1	
COL18A1		ITIH2	
COL14A1		SERPINA1C;1A	
COL12A1		PF4	

Not statistically significant (p>0.01) between dSPL vs dECM

Proteins common between dSPL and dECM		Proteins present in dSPL only	Proteins present in dECM only
Name	Name	Name	Name
EFEMP1	LOX	DPT	EFEMP2
MATN2	ADAMTSL4	FGL2	TSKU
EMILIN1	P4HA1	LTBP2	VCAN
FBN1	SERPINH1	MFAP4	COL4A5
POSTN	CTSB	MFAP5	COL4A6
LAMB2	LGALS3	VTN	CTSL
LAMC1	COLEC12	VWA1	PLOD3
LAMA5	ANXA2	LUM	SERPINF1
TNXB	ANXA5	OGN	NGF
NID2	LGALS9	CTSG	S100A6
PRELP	S100A4	ELANE	
BGN	ANGPTL2	SERPINA1B	
COL5A1	HCFC1	SERPINA1D	
COL16A1	PLXNB2	SERPINA1E	
COL1A1		SERPINA3K	
COL5A2		ANXA7	
COL1A2		LMAN1	
COL6A3		IL16	
COL4A1		S100A10	
COL6A2		S100A13	
COL6A1		S100A9	
COL4A2		TGFB1	

Glycoproteins
Proteoglycans
Collagens
ECM Regulators
ECM Affiliated
Secreted factors